



Article

# PI3K-AKT Pathway Modulation by Thymoquinone Limits Tumor Growth and Glycolytic Metabolism in Colorectal Cancer

Shahid Karim <sup>1,\*</sup>, Abdulhadi S. Burzangi <sup>1</sup>, Aftab Ahmad <sup>2</sup> , Nasir Ali Siddiqui <sup>3</sup> , Ibrahim M. Ibrahim <sup>1</sup> , Priyanka Sharma <sup>4</sup>, Walaa A. Abualsunun <sup>5</sup> and Gamal A. Gabr <sup>6,7</sup>

<sup>1</sup> Department of Pharmacology, Faculty of Medicine, King Abdulaziz University, Jeddah 21589, Saudi Arabia; burzangi@kau.edu.sa (A.S.B.); imibrahim1@kau.edu.sa (I.M.I.)

<sup>2</sup> Health Information Technology Department, Faculty of Applied Studies, King Abdulaziz University, Jeddah 21589, Saudi Arabia; abdul salam@kau.edu.sa

<sup>3</sup> Department of Pharmacognosy, College of Pharmacy, King Saud University, Riyadh 11451, Saudi Arabia; nasiratksu@gmail.com

<sup>4</sup> Center for Innovation in Personalized Medicine, King Fahad Medical Research, King Abdulaziz University, Jeddah 21589, Saudi Arabia; aamrahs@kau.edu.sa

<sup>5</sup> Department of Pharmaceutics, Faculty of Pharmacy, King Abdulaziz University, Jeddah 21589, Saudi Arabia; wabuassonon@kau.edu.sa

<sup>6</sup> Department of Pharmacology and Toxicology, College of Pharmacy, Prince Sattam Bin Abdulaziz University, Al-Kharj 11942, Saudi Arabia; g.gabr@psau.edu.sa

<sup>7</sup> Agricultural Genetic Engineering Research Institute, Agriculture Research Center, Giza 12619, Egypt

\* Correspondence: skaled@kau.edu.sa



**Citation:** Karim, S.; Burzangi, A.S.; Ahmad, A.; Siddiqui, N.A.; Ibrahim, I.M.; Sharma, P.; Abualsunun, W.A.; Gabr, G.A. PI3K-AKT Pathway Modulation by Thymoquinone Limits Tumor Growth and Glycolytic Metabolism in Colorectal Cancer. *Int. J. Mol. Sci.* **2022**, *23*, 2305. <https://doi.org/10.3390/ijms23042305>

Academic Editors: Adam Matkowski and Slavko Komarnytsky

Received: 6 January 2022

Accepted: 16 February 2022

Published: 19 February 2022

**Publisher's Note:** MDPI stays neutral with regard to jurisdictional claims in published maps and institutional affiliations.



**Copyright:** © 2022 by the authors. Licensee MDPI, Basel, Switzerland. This article is an open access article distributed under the terms and conditions of the Creative Commons Attribution (CC BY) license (<https://creativecommons.org/licenses/by/4.0/>).

**Abstract:** Colorectal cancer (CRC) is the third leading cause of death in men and the fourth in women worldwide and is characterized by deranged cellular energetics. Thymoquinone, an active component from *Nigella sativa*, has been extensively studied against cancer, however, its role in affecting deregulated cancer metabolism is largely unknown. Further, the phosphoinositide 3-kinase (PI3K) pathway is one of the most activated pathways in cancer and its activation is central to most deregulated metabolic pathways for supporting the anabolic needs of growing cancer cells. Herein, we provide evidence that thymoquinone inhibits glycolytic metabolism (Warburg effect) in colorectal cancer cell lines. Further, we show that such an abrogation of deranged cell metabolism was due, at least in part, to the inhibition of the rate-limiting glycolytic enzyme, Hexokinase 2 (HK2), via modulating the PI3/AKT axis. While overexpression of HK2 showed that it is essential for fueling glycolytic metabolism as well as sustaining tumorigenicity, its pharmacologic and/or genetic inhibition led to a reduction in the observed effects. The results decipher HK2 mediated inhibitory effects of thymoquinone in modulating its glycolytic metabolism and antitumor effects. In conclusion, we provide evidence of metabolic perturbation by thymoquinone in CRC cells, highlighting its potential to be used/repurposed as an antimetabolite drug, though the latter needs further validation utilizing other suitable cell and/or preclinical animal models.

**Keywords:** thymoquinone; Warburg effect; antimetabolite; colorectal cancer

## 1. Introduction

Tumor cells are supported by metabolic rewiring in their growth, proliferation, survival, maintenance and reprogram the pathways of nutrient acquisition to meet the bioenergetics [1]. This metabolic reprogramming is known as one of the prominent hallmarks of almost all cancers [2]. The hypothesis that cancer cells uptake glucose and produce a significant amount of lactate in the presence of normoxia due to weak mitochondrial function led to the broadly held delusion that cancer cells follow glycolysis as their major source of ATP [3]. Many tumor cells reside in nutrient and oxygen-deficient environments, which makes a heterogeneous build-up that led cancer cells to adopt several methods to sustain mitochondrial function for survival [4]. Metabolism is improved in differentiated

non-dividing cells to supply ATP through OXPHOS. Cells that proliferate at faster rates whether tumor cells or normal embryonic, immune and regenerating cells need ATP as well as anabolic constructive material for biomass improvement and nutrient refilling [5,6]. A glycolytic fermentative constitution similar to tumor cells is displayed by highly proliferative normal cells as well; a major division in cancer cells is the loss of the regulatory response kink [7]. This exclusive glucose-dependent phenotype together with enhanced lactate tumors serving as potential biomarkers of poor patient survival has motivated us along with other scientists [8–11] to disengage glycolysis in cancers as a presumed therapeutic move.

In human cancers, the most commonly activated pathway is said to be the phosphoinositide 3-kinase PI3K-AKT pathway [12]. This pathway renovated cellular metabolism in cancer cells by increasing the action of nutrient transporters and metabolic enzymes by oncogenic activation following the anabolic demands of abnormally growing cells. It was reported that the PI3K pathway controls the reprogramming of hexokinases (HKs), the enzymes which play a potent role in the conversion of glucose into glucose-6-phosphate (a major rate-limiting stage of glycolysis) and other metabolic pathways which lead to the up-regulation of HK II expression [13,14].

In glucose metabolism, the catalysis loyalty is started by Hexokinases (HKs). Glucose transporters (GLUTs) transport glucose via the plasma membrane and are phosphorylated by Hexokinases to produce glucose-6-phosphate [15]. In humans, four isoforms of Hexokinases were categorized which are HK: I, II, III and IV. Being structurally similar, the four isoforms vary in expression pattern, cellular localization and properties in regulation. The dominantly expressed among these is HK II which is found to be up-regulated in most of the tissues [16]. Hexokinase II was found to be over-expressed in most cancers leading to enhanced glycolytic rate, which is a phenotype for cancer cells [17]. Many studies have suggested HK II as a therapeutic target for treating cancer [18,19]. Therefore, it is important to evaluate compounds/drugs that could be effective in repressing HK II and hence could inhibit tumor metabolism.

Thymoquinone (TQ), also known as black seed or black cumin, is a key bioactive phytochemical constituent of *Nigella sativa* and it plays a major role in providing health benefits via anti-oxidant, anti-microbial, anti-diabetic, anti-inflammatory effects, metabolic syndrome disorders and has a long history of medicinal use in traditional medicinal practices [20–23]. Many studies have established TQ as a potential anti-cancer agent by inhibiting proliferation, migration, invasion and angiogenesis in a variety of cancer cells [24]. Thymoquinone targets cancer signaling molecules and pathways through different axes in various cancers. In prostate cancer thymoquinone targets via the down-regulation of the androgen receptor (AR) and the proliferation regulator E2F-1 [25]; the (STAT3) pathway in human multiple myeloma cells [26]; JAK2 and c-Src in gastric cancer cells [27]; Bax up-regulation, Bcl-2 inhibition and activation of caspases in colorectal cancer [28]; inhibiting p38 MAPK in oral cancer [29]; activating p73 and UHRF1-dependent mitochondrial and cell cycle checkpoints in acute lymphoblastic leukemia [30,31], and the inhibition of the Notch signaling pathway in hepatic carcinoma [32]. On the other hand, the effect of thymoquinone on cancer metabolism, an emerging hallmark of cancer, is unclear.

In the present study, we investigated the effect of thymoquinone in modulating PI3K-AKT/HK2-mediated deregulated cellular energetics in colorectal cancer (CRC) cells. We report for the first time that TQ inhibits HK2-mediated glycolytic metabolism, otherwise necessary to fuel the proliferation, clonogenicity and metastatic predisposition of CRC cells. Taken together, the data from the present study reveal the novel anticancerous potential of TQ by modulating cellular energetics, at least in part, via the PI3K-AKT/HK2 pathway.

## 2. Results

### 2.1. Thymoquinone Induces Cell Death in CRC Cells

Our first aim was to study the effect of thymoquinone on the growth inhibition against two human colorectal cancer cells lines, HCT116 and SW480. It was observed that treating

the cells with increasing concentrations of thymoquinone (0–100  $\mu\text{M}$ ) led to a dose and/or time-dependent reduction in cell viability (Figure 1A). The corresponding  $\text{IC}_{50}$  values for HCT116 and SW480 at 24 h (post-treatment) were 21.71  $\mu\text{M}$  and 20.53  $\mu\text{M}$ , and those at 48 h (post-treatment) were 10.26  $\mu\text{M}$  and 10.50  $\mu\text{M}$ , respectively, (Figure 1A,B). The lowest: highest percent death induction in HCT116 and SW480 at 24 h (post-treatment) was  $20.35 \pm 4.01$ ;  $74.95 \pm 5.39$  and  $17.71 \pm 3.87$ ;  $76.67 \pm 4.16$  while at 48 h (post-treatment) it was  $44.87 \pm 4.38$ ;  $88.30 \pm 6.26$  and  $48.04 \pm 4.47$ ;  $87.13 \pm 6.18$ , respectively. We also evaluated cell death over a time period of 1–4 days by employing a trypan blue dye exclusion assay; the results were consistent with MTT results showing more cell death/inhibition in cell doublings per day with the increase in drug concentration (Figure 1B). We did not evaluate TQ's biocompatibility on normal intestinal cells because the same was previously reported to be well tolerated by normal intestinal cells for concentrations of up to 60  $\mu\text{M}$  [33].

### 2.2. Thymoquinone Modulates Glycolytic Metabolism in CRC Cells

Deregulated cellular metabolism is a characteristic feature of most, if not all, cancerous cells and an emerging cancer hallmark [34,35], which expedites the cell-autonomous proliferation and survival of these cells [36]. The Warburg effect manifests an aberrant metabolic state in which cancer cells ferment glucose at higher rates to sustain the higher energy needs as well as biomass production, and hence ensure increased proliferation [5,37]. To this end, we speculated on studying whether cell death induced by TQ in CRC cells (HCT116 and SW480) could be attributed to the inhibition of the glycolytic phenotype in these cells. We found that sub-lethal doses of TQ in both HCT116 (21.71  $\mu\text{M}$ ) and SW480 (20.53  $\mu\text{M}$ ) after 24 h of treatment significantly reduced the glucose fermentation potential of these cells (Figure 2A). Additionally, such reduction in glucose fermentation capacity also led to a significant reduction in overall ATP production as well as maintaining the redox state (NADPH production) of these cells (Figure 2B,C). These results demonstrate that TQ-induced cell death and/or proliferation inhibition in CRC could be attributed to modulation of the glucose metabolic reprogramming, otherwise necessary to ensure increased biomass production and maintaining redox balance for sustaining proliferative signaling.

Since uncontrolled cell proliferation is a well-established cancer hallmark [2], we next attempted to evaluate whether sub-lethal dose/s of TQ have any modulatory effect on the proliferation index of CRC cells. It was observed that pre-treatment of TQ in both HCT116 (21.71  $\mu\text{M}$ ) as well as SW480 (20.53  $\mu\text{M}$ ) cells for 24 h led to a significant reduction in proliferation rate over time (0–4 days) (Figure 1C), highlighting its potential anti-proliferative role against CRC.

### 2.3. Thymoquinone Inhibits Hexokinase 2 via Modulating the PI3K-AKT Pathway

To underpin the role behind the reduction in the glucose fermentation rate in TQ-treated CRC cells, we evaluated the expression status of HK2, the first rate-limiting enzyme of glucose metabolism and an enzyme highly overexpressed in most cancers including CRC [38–41]. It was observed that TQ treatment substantially inhibited HK2 expression in HCT116 and SW480 cells (Figure 3A). Further, to know the mechanism behind the HK2 reduction, we evaluated the PI3K-AKT levels because previously it was reported that PI3K-AKT induces glycolytic phenotype via HK2 in pediatric osteosarcomas [13]. Expectedly, the reduction in HK2 levels upon TQ treatment coincided with significant inhibition in PI3K-AKT activation (i.e., reduction in p-PI3K-p-AKT<sup>T308/S473</sup>) (Figure 3B), suggesting that TQ inhibits HK2 via modulating the PI3K-AKT pathway. To confirm whether such reduction in HK2 was PI3K-AKT-dependent, we used the selective pharmacologic inhibitor (LY294002) of PI3K and we observed a significant reduction in HK2 levels concomitant to PI3K-AKT inhibition (Figure 3C). These results demonstrate that TQ inhibits glycolytic metabolism in CRC cells by inhibiting HK2 via the PI3K-AKT pathway.

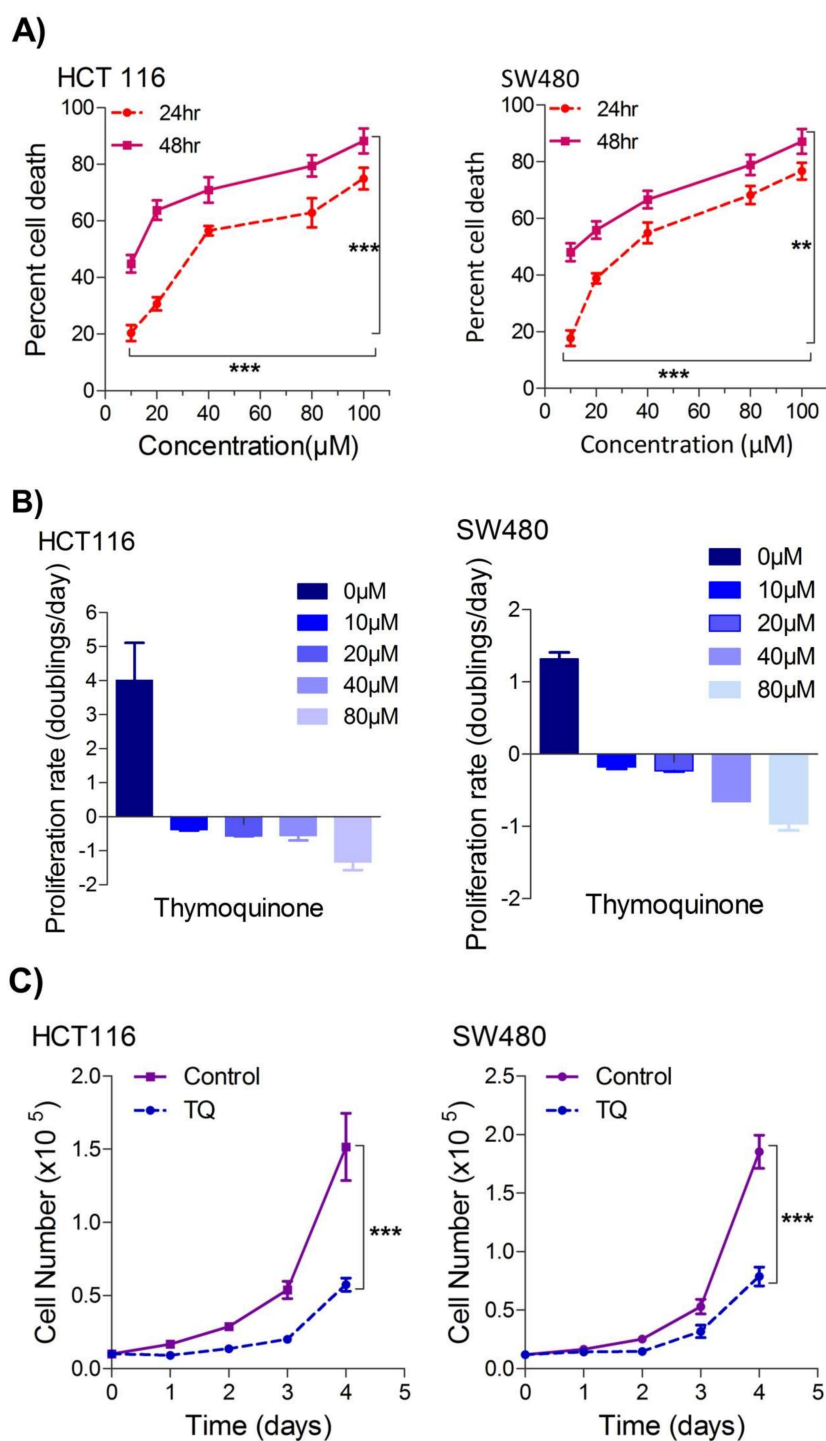


**Figure 1.** Thymoquinone induces cell death and hampers cell proliferation in CRC cells. HCT116 and SW480 CRC cells were treated with thymoquinone as indicated. (A) Thymoquinone induced cell death in a dose and time-dependent manner, statistical significance was calculated by two-way ANOVA, considering both time and concentration-dependent observations. (B) Thymoquinone treatment-induced cell death/inhibited cell doublings per day over a time period of 1–4 days. (C) Pre-treatment of thymoquinone to HCT116 (21.71  $\mu\text{M}$ ) and SW480 (20.53  $\mu\text{M}$ ) led to a significant reduction in cell proliferation over time (0–4 days), statistical significance was calculated by employing two way ANOVA following appropriate post hoc test (Bonferroni test). The results are expressed mean  $\pm$  SEM ( $n = 3$  or 4). \*\*  $p < 0.01$ , \*\*\*  $p < 0.001$ .

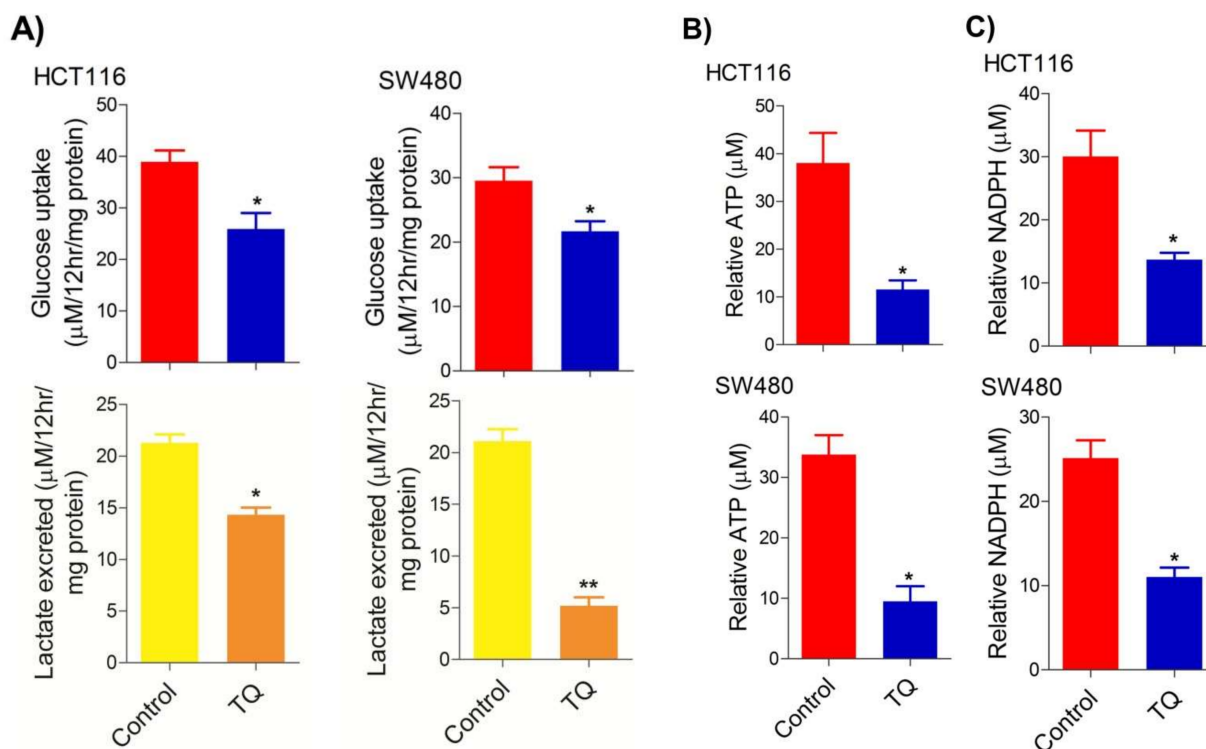


**Figure 2.** Thymoquinone reduces glycolytic metabolism in CRC. HCT116 and SW480 CRC cells were treated with thymoquinone as indicated. Thymoquinone treatment led to a significant reduction in—(A) glucose fermentation rate/s (glucose production and/or lactate production), (B) ATP production, and (C) redox state (NADPH) in these cells. Statistical significance was calculated by employing unpaired t-test, data expressed as mean  $\pm$  SEM ( $n = 3$ ). \*  $p < 0.05$  and \*\*  $p < 0.01$ .

#### 2.4. Inhibition of the PI3K-AKT/HK2 Pathway Abrogates the Tumorigenic Potential of CRC Cells

To seek whether targeting the PI3K-AKT/HK2 pathway also abrogates the tumorigenic propensity of CRC cells, we used a selective pharmacologic inhibitor of PI3K (LY294002) to study colony formation and cell proliferation over time. It was found that PI3K inhibition significantly inhibited colony formation potential as well as proliferation over time (Figure 4A,B); further confirming that the carcinogenic propensity of CRC cells (HCT116 and SW480) is majorly regulated via the PI3K-AKT axis. More importantly, genetic (siRNA) and low-dose pharmacologic (10  $\mu$ M, 3-Bromopyruvate) ablation of HK2 led to a significant reduction in cell proliferation as well as colony formation propensity in these cells (Figure 4C,D). Additionally, pharmacologic silencing of PI3K also led to a significant rescue in glycolytic reprogramming (Figure 4E–G), similarly, genetic ablation (siRNA-mediated) of HK2 also showed a significant reduction in glucose fermentation, ATP and NADPH production rates (Figure 4H–J). These results demonstrate that PI3K-AKT/HK2 activity directly regulates the tumorigenic propensity of CRC cells, which can be effectively targeted by TQ.

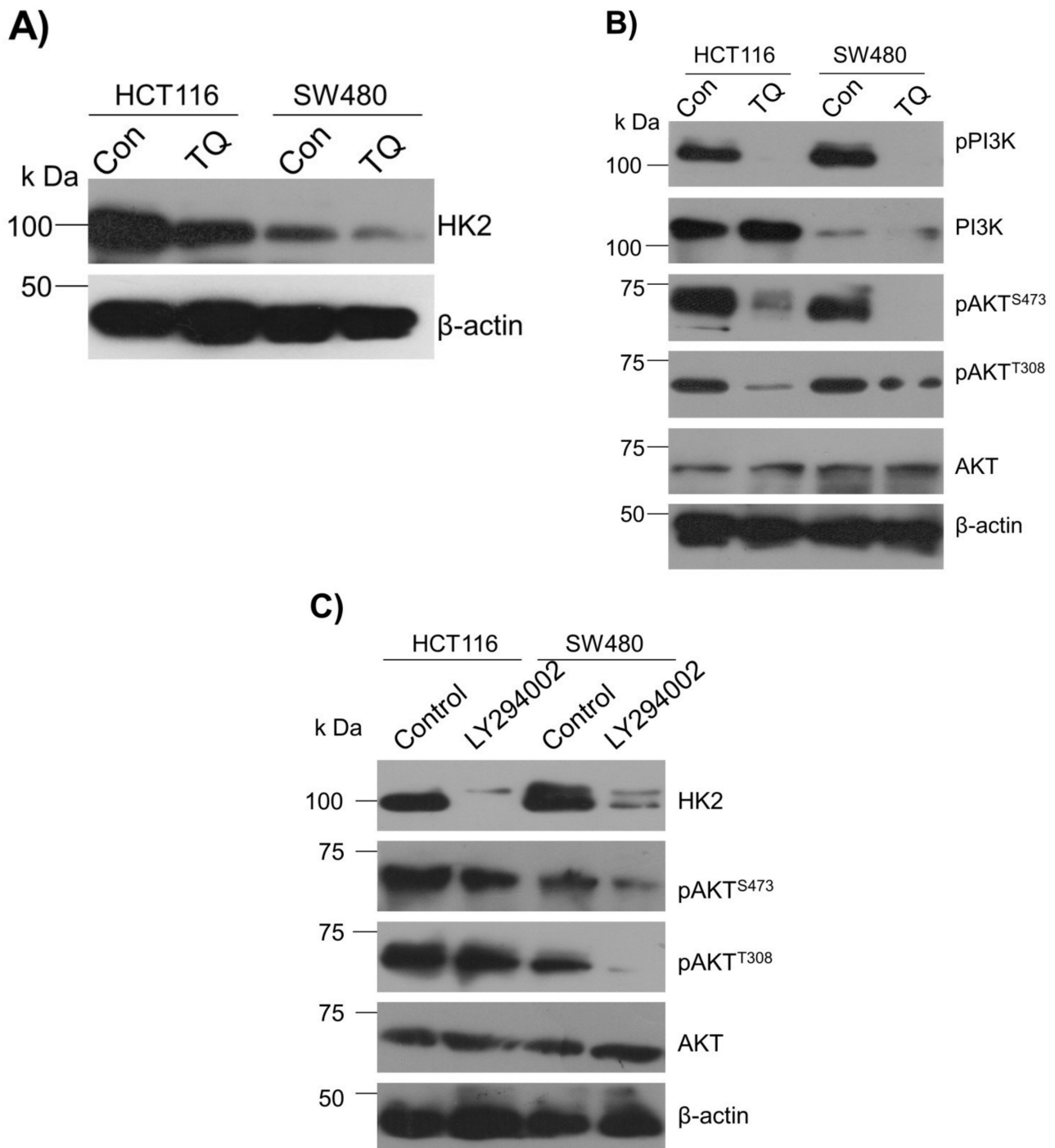


**Figure 3.** Thymoquinone inhibits Hexokinase-2 via modulating the PI3K-AKT pathway. HCT116 and SW480 CRC cells were treated with thymoquinone or LY294002 as indicated. (A) Thymoquinone treatment led to inhibition in HK2 protein levels. Such inhibition in HK2 was concomitant to inhibition in—(B) the PI3K-AKT pathway. (C) Inhibiting the PI3K-AKT pathway using selective PI3K pharmacologic inhibitor LY294002 led to an inhibition of HK2 protein levels.

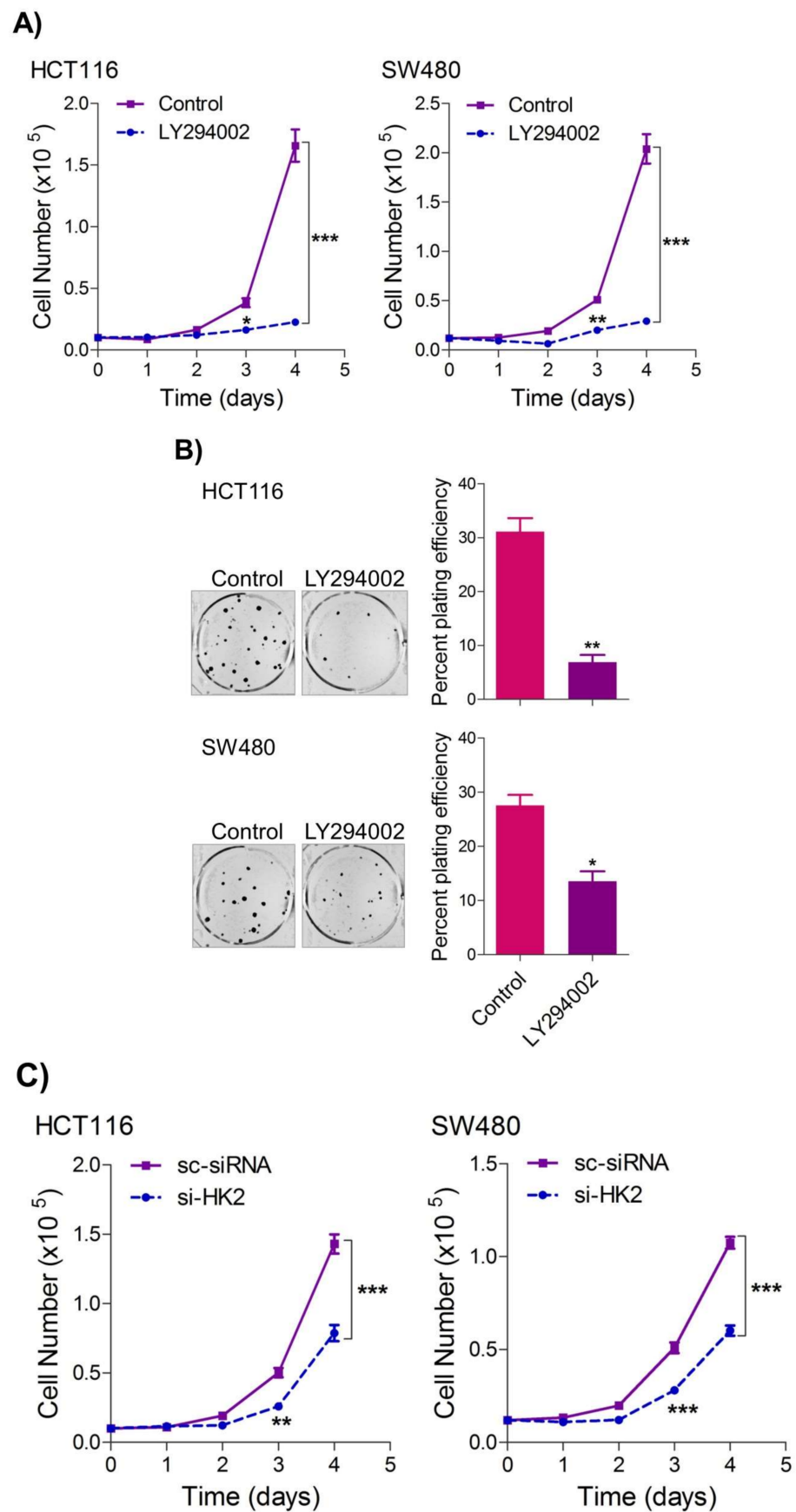
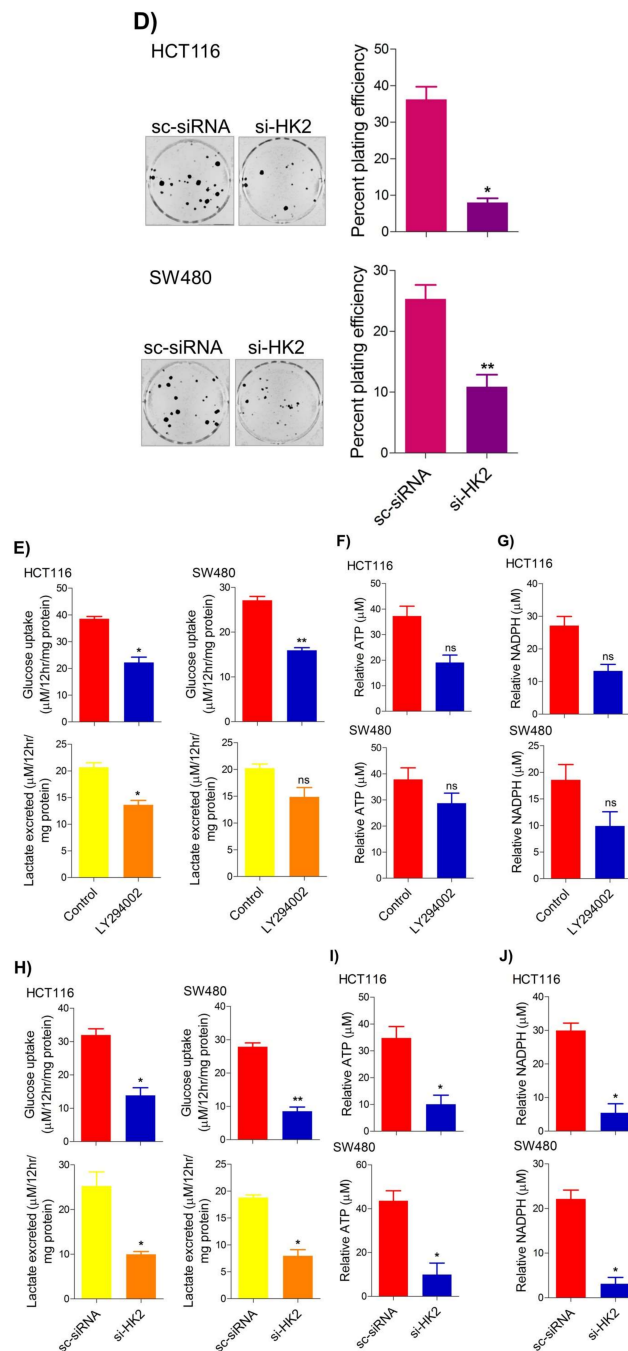


Figure 4. Cont.



**Figure 4.** Inhibition of PI3K-AKT/ HK2 pathway impedes tumorigenic potential of CRC cells. HCT116 and SW480 CRC cells were treated as indicated. Inhibition of PI3K with its pharmacologic inhibitor LY294002 led to a significant inhibition in—(A) cell proliferation, and (B) clonogenic propensity of these cells. Genetic (siRNA) or pharmacologic (3-Bromopyruvate) inhibition of HK2 led to a significant reduction in—(C) proliferation, and (D) Clonogenic potential of these cells. Statistical analyses were carried out employing two-tailed paired *t*-test (proliferation assays) and two-way ANOVA-(Clonogenic assays) followed by appropriate post hoc tests (Bonferroni). Pharmacologic (LY294002) inhibition of PI3K led to an inhibition in (E) glucose fermentation rate/s (glucose uptake and lactate excretion), (F) ATP production and (G) redox state (NADPH). Genetic (siRNA) ablation of HK2 led to a significant abrogation in (H) glucose fermentation rate/s (glucose uptake and lactate excretion), (I) ATP production and (J) redox state (NADPH). Statistical significance was calculated by employing unpaired *t*-test, data expressed as mean  $\pm$  SEM ( $n = 3$  or 4). \*  $p < 0.05$ , \*\*  $p < 0.01$ , \*\*\*  $p < 0.001$ .



### 2.5. Thymoquinone Inhibits Cell Migration and Invasion via Modulating Glucose Metabolic Reprogramming

Metastatic dissemination is one of the potent hallmarks of cancer [2], and with glucose metabolic reprogramming having a strong role in metastatic dissemination [9,42], our next interest was to seek whether and how thymoquinone impacts metastasis in CRC cells. To this end, we found that TQ treatment significantly inhibited the wound healing propensity and invasiveness of HCT116 and SW480 cells (Figure 5A,B), indicating its anti-metastatic potential. At the molecular level, TQ was able to induce E-cadherin while inhibiting N-cadherin expression (Figure 5C). Further, to confirm whether such inhibition in metastatic propensity was through glucose metabolic reprogramming, we employed genetic ablation of HK2 to inhibit the glucose uptake and hence glycolysis, which was found to rescue both wound healing as well as invasiveness in HCT116 and SW480 cells (Figure 5D,E). At the molecular level, such inhibition in glycolysis led to the induction of E-cadherin with a concomitant inhibition in N-cadherin levels (Figure 5F). Taken together, these data suggest that TQ inhibits metastatic predisposition of CRC cells, possibly via modulation of glucose metabolic reprogramming.

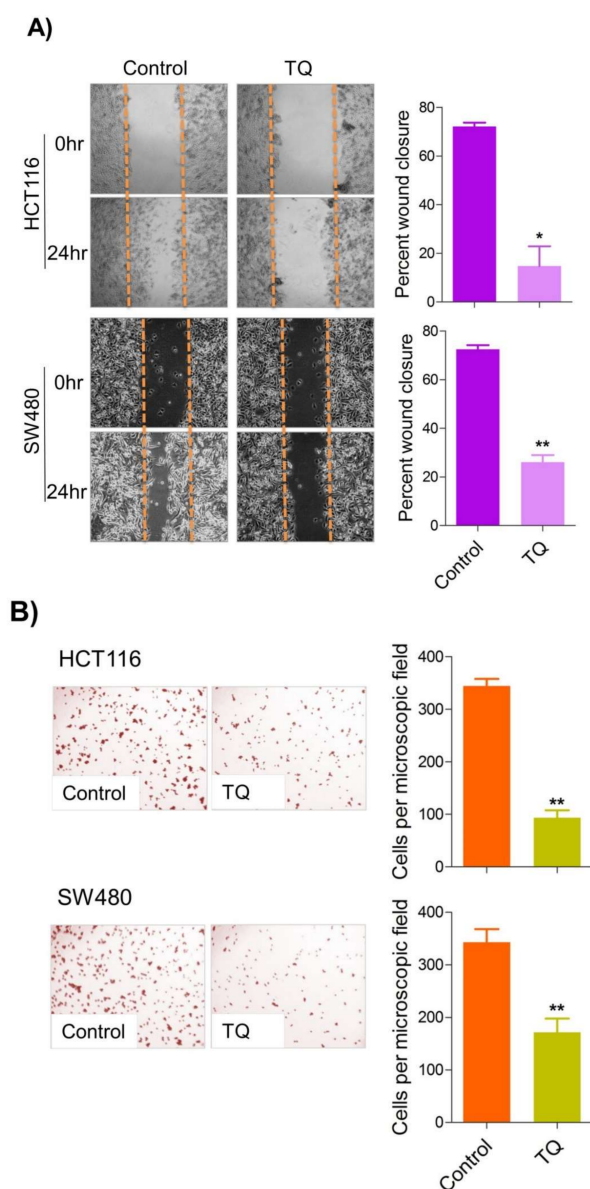
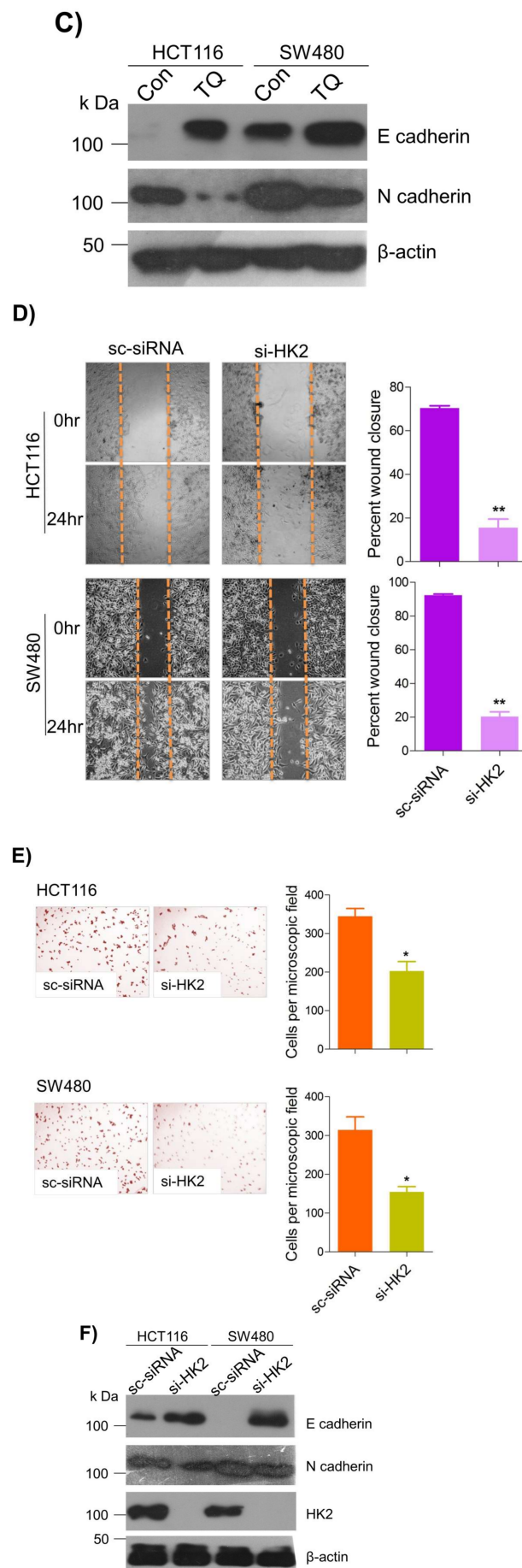


Figure 5. Cont.



**Figure 5.** Thymoquinone inhibits cell migration and invasion via modulating glucose metabolic

reprogramming. HCT116 and SW480 CRC cells were treated as indicated. Treating these cells with thymoquinone led to a significant inhibition in—(A) wound healing, and (B) invasion potential. (C) Thymoquinone also led to induction in E cadherin with a concomitant inhibition in N cadherin levels. Genetic (siRNA) ablation of HK2 led to a significant inhibition in—(D) wound healing, and (E) cell invasion. (F) HK2 ablation also led to induction in E cadherin and inhibition in N cadherin levels. Statistical analyses were carried out by employing two-tailed paired *t*-test, data expressed as mean  $\pm$  SEM ( $n = 3$ ). \*  $p < 0.05$ , \*\*  $p < 0.01$ .

### 3. Discussion

Though a substantial advancement has been achieved in CRC treatment due to scientific advancements in the past 10–15 years, it still remains one of the major causes of deaths due to cancer globally [43,44], besides being the most prevalent disease in the young (below 50 years of age) in more advanced stages [45]. No doubt many efforts are underway towards improving the systemic treatment of patients with metastatic colorectal cancer (m-CRC). Glucose metabolic reprogramming along with the aberrant tumor microenvironment (TME) has posed a challenge to effectively target the disease progression [46]. The “Warburg effect” or “aerobic glycolysis”, which is considered an important metabolic driver in the development of most solid cancers including CRC, leads to perturbations in the way cells consume nutrients to drive metabolic pathways [5,47]. Such aberrant glucose uptake and lactate production ensure higher anabolic needs of aberrantly proliferating CRC cells besides acidifying the tumor microenvironment (TME) to induce angiogenesis [5,48], metastatic dissemination [49,50], chemotherapeutic resistance [51,52] and immune evasion [53–55]. Such aberrant metabolic signatures not only provide growth advantages but also offers a therapeutic modality to selectively target such abnormal cells [56,57]. In this regard, various antimetabolite drugs were discovered that have shown a significant reduction in tumor burden by selectively targeting the aberrantly behaving metabolic enzymes/pathways [58–66], and many are undergoing clinical trials. Many phyto-compounds were reported to inhibit cancer growth [67,68] and cancer cell metabolism [8,69], highlighting the need to screen and study more phyto-compounds against cancer. To this end, we evaluated if and how TQ, a well-studied anticancer [70,71] (reviewed in [72]) secondary plant metabolite, modulates glycolytic phenotype in CRC cells. We found that TQ inhibits cell proliferation, clonogenicity and epithelial-mesenchymal transition (EMT) in CRC cells (HCT116 and SW480) and such inhibition is attributed to its role in modulating glycolytic metabolism of these cells. Mechanistically, TQ’s anti-carcinogenic potential is attributed to its inhibitory effects on the rate-limiting glycolytic enzyme HK2, leading to a reduction in glucose fermentation rate and hence inducing energy debt and dis-balancing the redox state of the proliferating CRC cells. Interestingly, such an anti-glycolytic effect was regulated at least in part via the PI3K-AKT pathway, the most aberrated pathway in cancer [12].

In human beings, HKs are a group of four (HK1-4) tissue-specific iso-enzymes that catalyze the first step (phosphorylation of glucose) in glucose metabolism [73]. However, the HK2 isoform is the critical regulator of the Warburg effect in many cancer types, viz prostate, hepatocellular, gliomas [39], breast [41], gastrointestinal [74], lung [63] and ovarian cancers [40,75], making it an important therapeutic target against cancer. TQ showed concentration-dependent cell death in HCT116 and SW480 cells (Figure 1), showing its potential as a cytotoxic agent capable of inhibiting cell proliferation in CRC. Such anticancer effects of TQ have previously been reported in various cancer models including CRC [24,76–80] with various modes of action. Though TQ is reported to induce cell death in renal cell carcinoma [81] and pancreatic cancers [82] via inhibiting HIF1 $\alpha$  and pyruvate kinase M2 (PKM2)-mediated glycolysis, further studies are warranted to elucidate the underlying mechanism/s using more cell models. Our results show for the first time that TQ-mediated proliferation arrest in CRC cells is attributed to its negative impact on the Warburg effect, otherwise necessary for the growth and proliferation of cancerous cells including CRC [5,9]. TQ treatment inhibited the glucose uptake and subsequent lactate production in HCT116 and SW480 cells, inducing a net energy debt and inhibiting the anabolic

metabolism, otherwise necessary to support macromolecule biosynthesis of highly proliferating cells. The decrease in HK2 expression levels explains the regulatory knot behind such inhibition of glucose fermentation, post-TQ treatment. The reduction in cell proliferation and/or clonogenicity, besides a rescue in glucose fermentation rate upon HK2 silencing (Figure 2), explains that such tumorigenic propensity in CRC cells is dependent on aberrant metabolic nature regulated, at least in part, via HK2.

The PI3K-AKT pathway is the most aberrant pathway in many cancers [12,83] including CRC (reviewed in [84,85]), which not only activates cell proliferation, growth metastasis but also induces apoptotic evasion. The PI3K-AKT was established to positively regulate the Warburg effect via increased glucose uptake as well as phosphorylation and activation of glycolytic enzymes (reviewed in [36]). Moreover, PI3K-AKT was also reported to induce the Warburg effect via up-regulating HK2 expression and tumorigenic growth in osteosarcoma [13]. Our results also confirmed that aberrant glucose fermentation rate and enhanced tumorigenicity in CRC cells may be attributed to activating the PI3K-AKT/HK2 axis besides some other oncogenic events [9], evidenced by direct inhibition of HK2 expression and tumorigenicity upon selectively inhibiting PI3K-AKT. In corroboration with our findings, constitutively active AKT was found to sufficiently trigger glycolysis [86,87], leading to increased uptake of glucose and glycolytic flux independent of growth factor signaling [86–91], thus rendering such cells to rely on glucose to survive [87,91]. To the best of our knowledge, results from the present study demonstrate for the first time that TQ induces proliferation arrest and cell death in CRC by inhibiting PI3K-AKT, which in turn inhibits HK2 and hence glucose uptake, subsequently leading to the ATP debt and inhibiting molecular building blocks otherwise necessary for continued proliferation and growth of cancerous cells [56,92]. More importantly, the reduction in the NADPH levels upon TQ treatment indicates an inhibition in reductive biosynthesis while inducing oxidative stress [36,93–95]. In similar lines, PI3K-AKT was known to regulate multiple checkpoints in the glycolytic pathway, viz post-translational as well as transcriptional gears on glucose transporter and/or other glycolytic enzymes [36].

Metastasis is a multistep process that is regulated by multiple factors and accounts for approximately 90% of cancer-related mortality across the world [96]. Epithelial-mesenchymal transition (EMT), an early metastasis step, is known for the dissemination of circulatory tumor cells (CTC's) into the bloodstream and accounts for the worse cancer prognosis [97–99]. Moreover, approximately 20% of newly detected CRC cancers are metastatic and about 20% more will transform into metastatic, accounting for lower survival rates [100,101]. In the present study, we found that TQ treatment to HCT116 and SW480 cells led to inhibition in cell invasion and concomitant induction of epithelial cell marker E-cadherin while down-regulating the mesenchymal marker N-cadherin. Furthermore, TQ treatment also abrogated the wound healing potential of these cells, further supporting its anti-metastatic effect of TQ [102,103]. Though TQ has previously been shown to show strong anti-metastatic effects [102,103], the mechanisms are still not very clear. The results from the present study provide evidence that anti-metastatic effects of TQ are mediated by a reduction in the glycolytic rate [9,104–106], which in turn modulates redox status and induces an energy crisis otherwise necessary for metastasizing cells. Such metabolic intervention by TQ was further confirmed upon inhibiting HK2-mediated phosphorylation of glucose (using the 3-bromopyruvate/ siRNA approach). Overall, the results from the present study underpin a novel mechanism of TQ against CRC progression by a reduction in the glycolytic rate, possibly mediated via the PI3K-AKT/HK2 axis (Figure 6). We suggest employing other cancers and/or employing suitable *in vivo* models in more advanced settings to decipher such anticancer effects of TQ.

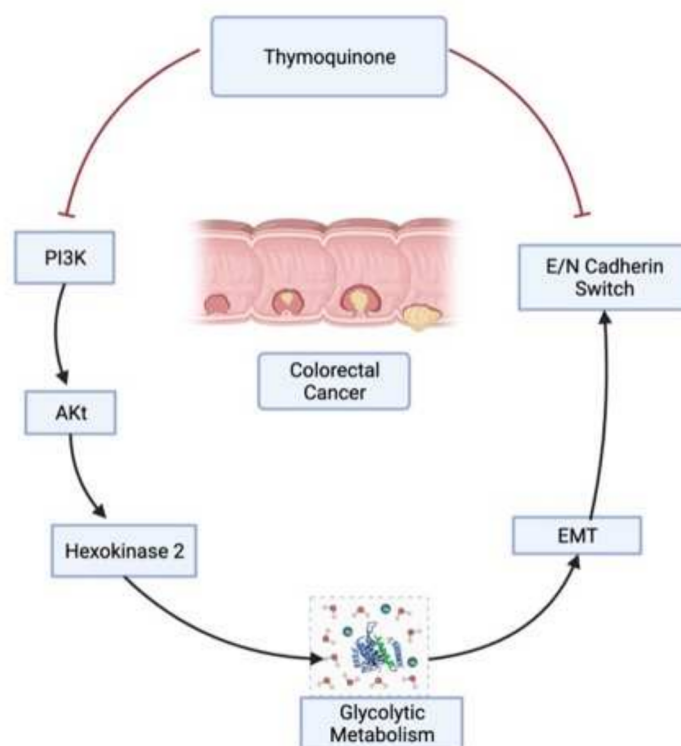


**Figure 6.** Overall mechanistic representation of thymoquinone in colorectal cancer.

#### 4. Materials and Methods

##### 4.1. Cell Lines

The study was conducted using two CRC cell lines, HCT116 and SW480, acquired from National Centre for Cell Sciences, Pune India (NCCS, Pune) India. Both the cell lines were grown in Dulbecco's Modified Eagles Medium (DMEM, Gibco) supplemented with 2-mM glutamine, 1 × pen/strep (Gibco) and 10% Fetal Bovine Serum (FBS, Gibco) at 37 °C temperature and 5% CO<sub>2</sub> under humid settings in a cell culture incubator (Shell labs).

##### 4.2. Cytotoxicity (MTT) and Cell Doubling Assays

MTT colorimetric test with thymoquinone was performed in CRC cell lines (HCT116 and SW480). For 24 h, we seeded  $3 \times 10^4$  HCT116 and SW480 in each well of a 96-well plate. The cells were subsequently incubated with increasing concentrations of thymoquinone (Selleckchem, Cat no.S4761) (0–100 µM). Following a 24-h incubation period, the treated samples were withdrawn from the wells and the cells were incubated for 4 h at 37 °C with 25 L of MTT solution (0.5%, *w/v*). The unreacted MTT solution was withdrawn after incubation, and the cells were exposed to 150 L DMSO (Selleckchem, Cat no. B14001) in each well for 20 min to solubilize the produced formazan crystals. Finally, using a microplate reader (Thermo Fisher Scientific, Waltham, MA, USA), the absorbance of the formazan solution in each well was measured at 570 nm; the absorbance was directly proportional to the number of viable cells in the wells.

The assay was performed to study the effect of TQ on cell doubling, as per previously described method with little modifications [107]. Briefly, the cells ( $1.0 \times 10^4$ ) cells were seeded in 12 well plates in triplicate and allowed to attach overnight. Next day the cells from one representative well were trypsinized to count them to get initial cell number, and rest wells treated with TQ and allowed to incubate for 4 days. The cells were counted after 4 days post-treatment, using Neubaur Chamber to calculate cell doubling as:

$$\text{Proliferation Rate (Doubling/day)} = \log_2 (\text{Final cell count (day 5)/cell count (day 1)/4 (days)}).$$

#### 4.3. Colony Formation Assay

The colony formation assay was performed to study the effect of indicated treatments/genetic modifications on cologenic potential of CRC cells, following the previously defined protocol with slight modification [9]. Briefly, the cells were either treated with low dose pharmacologic inhibitor of PI3K (LY294002) for 48 h at which time the cells were trypsinized and seeded at a density of 200 cells/6-well in triplicate and allowed to grow for 3–4 weeks until individual colonies became visible. Then the media was removed out and cells were stained with 0.1% crystal violet for half an hour, followed by gentle rinsing in still tap water until excess dye was washed out. After washing, the plates were scanned on white background using Chemodoc XRS+ from Bio Rad to count the visible cell colonies in different groups and calculate the plating efficiency. Plating efficiency was similarly performed post HK2 silencing using siRNA gene silencing approach.

#### 4.4. Cell Proliferation Assay

The low passage healthy cells were seeded in 60 mm dishes at  $6.5\text{--}7.5 \times 10^5$  cell density and treated next day with  $IC_{50}$  concentration of TQ or low dose LY294002 (PI3K inhibitor) for 36 h at which time the cells were trypsinized and seeded in 12 well plates at a density ranging from  $1.0 \times 10^4\text{--}1.5 \times 10^4$  cells per well in 4 replicates in quadruplet (1–4). Each day, a couple of wells from each treatment group were trypsinized and counted manually; using a Neubauer chamber and a growth curve was generated over a period of 96 h. For HK2 inhibition, siRNA transfected cells along with corresponding mocks (sc-siRNA groups) were seeded after 40–48 h post-transfection and the proliferation evaluated as above.

#### 4.5. Colony Formation Assay

##### siRNA Transfection

siRNA transfections were given transiently for control siRNA (sc-siRNA), sense-UUCUCCGAACGUGUCACGUTT anti sense-ACGUGACACGUUCGGAGAATT oligos (IDT), sequences described previously [108], and predesigned silencer select HK2 siRNA, Thermo (ID:144506; AM16708) using Lipofectamine RNAi max reagent (Thermo scientific) as per manufacturer instructions following our previously reported procedure with slight modifications [9]. Briefly, the cells at around 70% confluence transfected with 20 nM of indicated Oligos after serum starving them for 4–5 h. The transfected cells were replenished with fresh media after 8 h and gene silencing was assessed after 72 h, post-transfection using Western blot. For cell proliferation, clonogenic, metabolic and/or metastasis-related assays the transfected cells were trypsinized at 48 h (post-transfection) and seeded at appropriate densities into 12 well or 35 mm dishes as needed.

#### 4.6. Wound Healing and Cell Invasion Assays

The wound-healing assay was carried out on HCT116 and SW480 cells for evaluating the cell migration, following previously described procedure with some modifications [9]. Briefly  $1.5\text{--}2 \times 10^5$  cells were seeded in 12 well plates in triplicate and allowed to grow to confluency (approx. >90%). After this, the cells were serum-starved for 7–8 h and scratches were made using a P10 tip, along the respective diameter of the wells. Then the media was gently aspirated and the detached cells washed off using  $1 \times$  PBS. The cells were then replenished with low serum (0.5%) cell culture media or low serum media along with 25  $\mu$ M TQ or 20  $\mu$ M 3-bromopyruvate (3-BP) as indicated. Images were taken at 0 and 24 h after scratch was made and the migratory propensity calculated in terms of wound closure in respective groups using Image J (NIH) software. Further, the cell invasion assay/s was carried out using transwell inserts, for which about  $1 \times 10^5$  cells were seeded in serum-free media (200  $\mu$ L) or 25  $\mu$ M TQ/20  $\mu$ M 3-BP in 24 well transwell inserts (SPL Insert; catalog 36224), coated with 40  $\mu$ L extracellular matrix (ECM). The complete growth media (600–700  $\mu$ L) containing 10% FBS was put in the lower chamber of the plate to serve as chemo-attractant and induce cells to pass across transwell pores. The cells were pretreated with indicated drugs (TQ or 3-BP) for 24 h before carrying out the cell invasion

assay/s. Similarly, pre-transfected (48 h before) si-HK2 groups were processed in the same way as above. After 24 h of incubation, the inserts were washed softly using 1X PBS, fixed in ice-cold ethanol (70%) for 15 min and then stained using 0.1% crystal violet dye for next 10–15 min. Finally, after de-staining in tape water, the wells were swabbed from inside to remove matrigel and noninvasive cells. Invasion efficiency was calculated by counting the cells in random fields, under microscope and representative images taken.

#### 4.7. Western Blot

The indicated cell groups were trypsinized and lysed in Pierce IP lysis buffer (Thermo Fisher Scientific) containing 0.5% sodium deoxycholate, 0.1% SDS and 1X Sigma fast (Sigma Aldrich) for 10–15 min on ice. The lysate was centrifuged at 10,000 rpm for 10 min at 4 °C. The supernatant was aspirated into fresh Eppendorf tubes and total protein quantified using BCA kit as per manufacturer instructions (Thermo Scientific). Equal amounts of protein (40–50 µg) were resolved on SDS PAGE and transferred onto PVDF membrane (Bio Rad) employing wet transfer at 75 V for 1.5 h at 4 °C. The membranes were probed with indicated primary antibodies overnight at 4 °C after blocking them in 5% skimmed milk (in 1× TBST) for 1 h. After 12 h of primary probing, the membranes were washed thrice for 5 min each in 1x TBST followed by secondary probing with appropriate HRP tagged secondary antibodies at room temperature for 1 h. The protein expression was observed using chemiluminescence-based detection on X-ray film (Amersham). The primary antibodies used were against β-actin (NB600-501, Novus Biologicals), E-cadherin (NBP2-19051, Novus Biologicals), N-cadherin (NBP1-48309, Novus Biologicals), HK2 (STJ99121, Saint Johns), pAKT<sup>S473</sup> (sc-293125, Santa Cruz), pAKT<sup>T308</sup> (sc-135650, Santa Cruz), pPI3K (4228S, Santa Cruz) and the corresponding secondary antibodies used were either goat anti-rabbit IgG-HRP (NB7160, Novus Biologicals) or goat anti-mouse IgG-HRP (NB7539, Novus Biologicals).

#### 4.8. Glucose Uptake/Lactate Production, ATP, and NADPH Measurement

Glucose uptake and lactate production was measured in the spent media using respective kits (Eton Bioscience, SKU-1200032002 and 1200012002) as per manufacturer instructions. Similarly, ATP levels were measured using ATP Colorimetric/ Fluorometric Kit (Bio vision, K354-100) and NADPH levels were quantified using Ampelite Colorimetric NADPH Assay Kit (AAT Bioquest, 15272) as per manufacturer instructions.

#### 4.9. Statistical Analyses

The statistical analyses were carried out using Graph Pad Prism V 5.0. The differences between groups were analyzed either by unpaired *t*-test or two-way ANOVA as applicable with appropriate post hoc tests as mentioned. All the data are represented as mean ± SEM of at least three replicates unless otherwise stated. *p* values corresponding to  $p \leq 0.05$  were considered statistically significant.

**Author Contributions:** Conceptualization, A.S.B. and S.K.; Data curation, A.A.; Formal analysis, W.A.A.; Funding acquisition, S.K.; Investigation, W.A.A.; Methodology, A.S.B., N.A.S. and I.M.I.; Project administration, S.K., N.A.S. and G.A.G.; Resources, N.A.S. and P.S.; Software, P.S.; Supervision, A.A. and I.M.I.; Validation, W.A.A.; Writing—original draft, A.S.B. and G.A.G.; Writing—review and editing, S.K., A.A. and G.A.G. All authors have read and agreed to the published version of the manuscript.

**Funding:** The Deanship of Scientific Research (DSR) at King Abdulaziz University, Jeddah, Saudi Arabia has funded this project, under grant no. (KEP-27-166-42).

**Institutional Review Board Statement:** Not applicable.

**Informed Consent Statement:** Not applicable.

**Data Availability Statement:** Not applicable.

**Conflicts of Interest:** The authors declare no conflict of interest.

## References

1. De Berardinis, R.J.; Chandel, N.S. Fundamentals of cancer metabolism. *Sci. Adv.* **2016**, *2*, e1600200. [[CrossRef](#)] [[PubMed](#)]
2. Hanahan, D.; Weinberg, R.A. Hallmarks of cancer: The next generation. *Cell* **2011**, *144*, 646–674. [[CrossRef](#)] [[PubMed](#)]
3. Warburg, O. On the origin of cancer cells. *Science* **1956**, *123*, 309–314. [[CrossRef](#)] [[PubMed](#)]
4. Chandel, N.S.; Budinger, G.R.; Choe, S.H.; Schumacker, P.T. Cellular respiration during hypoxia. Role of cytochrome oxidase as the oxygen sensor in hepatocytes. *J. Biol. Chem.* **1997**, *272*, 18808–18816. [[CrossRef](#)] [[PubMed](#)]
5. Vander Heiden, M.G.; Cantley, L.C.; Thompson, C.B. Understanding the Warburg effect: The metabolic requirements of cell proliferation. *Science* **2009**, *324*, 1029–1033. [[CrossRef](#)] [[PubMed](#)]
6. Palm, W.; Thompson, C.B. Nutrient acquisition strategies of mammalian cells. *Nature* **2017**, *546*, 234–242. [[CrossRef](#)] [[PubMed](#)]
7. Kroemer, G.; Pouyssegur, J. Tumor cell metabolism: Cancer’s Achilles’ heel. *Cancer Cell* **2008**, *13*, 472–482. [[CrossRef](#)] [[PubMed](#)]
8. Siddiqui, F.A.; Prakasam, G.; Chattopadhyay, S.; Rehman, A.U.; Padder, R.A.; Ansari, M.A.; Irshad, R.; Mangalhari, K.; Bamezai, R.N.K.; Husain, M.; et al. Curcumin decreases Warburg effect in cancer cells by down-regulating pyruvate kinase M2 via mTOR-HIF1 $\alpha$  inhibition. *Sci. Rep.* **2018**, *8*, 8323. [[CrossRef](#)] [[PubMed](#)]
9. Padder, R.A.; Bhat, Z.I.; Ahmad, Z.; Singh, N.; Husain, M. DRP1 Promotes BRAFV600E-Driven Tumor Progression and Metabolic Reprogramming in Colorectal Cancer. *Front. Oncol.* **2021**, *10*, 592130. [[CrossRef](#)] [[PubMed](#)]
10. Fadaka, A.; Ajiboye, B.; Ojo, O.; Adewale, O.; Olayide, I.; Emuowhochere, R. Biology of glucose metabolism in cancer cells. *J. Oncol. Sci.* **2017**, *3*, 45–51. [[CrossRef](#)]
11. Parks, S.K.; Mueller-Klieser, W.; Pouyssegur, J. Lactate and Acidity in the Cancer Microenvironment. *Annu. Rev. Cancer Biol.* **2020**, *4*, 141–158. [[CrossRef](#)]
12. Lawrence, M.S.; Stojanov, P.; Mermel, C.H.; Robinson, J.T.; Garraway, L.A.; Golub, T.R.; Meyerson, M.; Gabriel, S.B.; Lander, E.S.; Getz, G. Discovery and saturation analysis of cancer genes across 21 tumour types. *Nature* **2014**, *505*, 495–501. [[CrossRef](#)]
13. Zhuo, B.; Li, Y.; Li, Z.; Qin, H.; Sun, Q.; Zhang, F.; Shen, Y.; Shi, Y.; Wang, R. PI3K/Akt signaling mediated Hexokinase-2 expression inhibits cell apoptosis and promotes tumor growth in pediatric osteosarcoma. *Biochem. Biophys. Res. Commun.* **2015**, *464*, 401–406. [[CrossRef](#)] [[PubMed](#)]
14. Marshall, A.J.; Mejia, E.; Hou, S.; Sher, A.; Hatch, G.; Aliani, M. PI3K-dependent Reprogramming of Hexokinase Isoforms Regulates B Lymphocyte Metabolism. *J. Immunol.* **2020**, *204* (Suppl. S1), 151.30.
15. Roberts, D.J.; Miyamoto, S. Hexokinase II integrates energy metabolism and cellular protection: Acting on mitochondria and TORCing to autophagy. *Cell Death Differ.* **2015**, *22*, 248–257. [[CrossRef](#)]
16. Nowak, N.; Kulma, A.; Gutowicz, J. Up-regulation of Key Glycolysis Proteins in Cancer Development. *Open Life Sci.* **2018**, *13*, 569–581. [[CrossRef](#)] [[PubMed](#)]
17. Gandham, S.K.; Talekar, M.; Singh, A.; Amiji, M.M. Inhibition of hexokinase-2 with targeted liposomal 3-bromopyruvate in an ovarian tumor spheroid model of aerobic glycolysis. *Int. J. Nanomed.* **2015**, *10*, 4405–4423. [[CrossRef](#)]
18. Xu, S.; Herschman, H.R. A Tumor Agnostic Therapeutic Strategy for Hexokinase 1-Null/Hexokinase 2-Positive Cancers. *Cancer Res.* **2019**, *79*, 5907–5914. [[CrossRef](#)] [[PubMed](#)]
19. Xu, S.; Catapang, A.; Braas, D.; Stiles, L.; Doh, H.M.; Lee, J.T.; Graeber, T.G.; Damoiseaux, R.; Shirihai, O.; Herschman, H.R. A precision therapeutic strategy for hexokinase 1-null, hexokinase 2-positive cancers. *Cancer Metab.* **2018**, *6*, 7. [[CrossRef](#)] [[PubMed](#)]
20. Padhye, S.; Banerjee, S.; Ahmad, A.; Mohammad, R.; Sarkar, F.H. From here to eternity—The secret of Pharaohs: Therapeutic potential of black cumin seeds and beyond. *Cancer Ther.* **2008**, *6*, 495–510. [[PubMed](#)]
21. Abdelmeguid, N.E.; Fakhoury, R.; Kamal, S.M.; Al Wafai, R.J. Effects of Nigella sativa and thymoquinone on biochemical and subcellular changes in pancreatic  $\beta$ -cells of streptozotocin-induced diabetic rats. *J. Diabetes* **2010**, *2*, 256–266. [[CrossRef](#)] [[PubMed](#)]
22. Razavi, B.M.; Hosseinzadeh, H. A review of the effects of Nigella sativa L. and its constituent, thymoquinone, in metabolic syndrome. *J. Endocrinol. Investig.* **2014**, *37*, 1031–1040. [[CrossRef](#)] [[PubMed](#)]
23. Balbaa, M.; El-Zeftawy, M.; Ghareeb, D.; Taha, N.; Mandour, A.W. Nigella sativa Relieves the Altered Insulin Receptor Signaling in Streptozotocin-Induced Diabetic Rats Fed with a High-Fat Diet. *Oxidative Med. Cell. Longev.* **2016**, *2016*, 2492107. [[CrossRef](#)] [[PubMed](#)]
24. Imran, M.; Rauf, A.; Khan, I.A.; Shahbaz, M.; Qaisrani, T.B.; Fatmawati, S.; Abu-Izneid, T.; Imran, A.; Rahman, K.U.; Gondal, T.A. Thymoquinone: A novel strategy to combat cancer: A review. *Biomed. Pharmacother.* **2018**, *106*, 390–402. [[CrossRef](#)] [[PubMed](#)]
25. Kaseb, A.O.; Chinnakannu, K.; Chen, D.; Sivanandam, A.; Tejwani, S.; Menon, M.; Dou, Q.P.; Reddy, G.P. Androgen receptor and E2F-1 targeted thymoquinone therapy for hormone-refractory prostate cancer. *Cancer Res.* **2007**, *67*, 7782–7788. [[CrossRef](#)] [[PubMed](#)]
26. Badr, G.; Mohany, M.; Abu-Tarboush, F. Thymoquinone decreases F-actin polymerization and the proliferation of human multiple myeloma cells by suppressing STAT3 phosphorylation and Bcl2/Bcl-XL expression. *Lipids Health Dis.* **2011**, *10*, 236. [[CrossRef](#)] [[PubMed](#)]
27. Zhu, W.Q.; Wang, J.; Guo, X.F.; Liu, Z.; Dong, W.G. Thymoquinone inhibits proliferation in gastric cancer via the STAT3 pathway in vivo and in vitro. *World J. Gastroenterol.* **2016**, *22*, 4149–4159. [[CrossRef](#)] [[PubMed](#)]
28. Kundu, J.; Choi, B.Y.; Jeong, C.H.; Kundu, J.K.; Chun, K.S. Thymoquinone induces apoptosis in human colon cancer HCT116 cells through inactivation of STAT3 by blocking JAK2- and Src-mediated phosphorylation of EGF receptor tyrosine kinase. *Oncol. Rep.* **2014**, *32*, 821–828. [[CrossRef](#)]



29. Abdelfadil, E.; Cheng, Y.H.; Bau, D.T.; Ting, W.J.; Chen, L.M.; Hsu, H.H.; Lin, Y.M.; Chen, R.J.; Tsai, F.J.; Tsai, C.H.; et al. Thymoquinone induces apoptosis in oral cancer cells through p38 $\beta$  inhibition. *Am. J. Chin. Med.* **2013**, *41*, 683–696. [[CrossRef](#)] [[PubMed](#)]
30. Alhosin, M.; Abusnina, A.; Achour, M.; Sharif, T.; Muller, C.; Peluso, J.; Chataigneau, T.; Lugnier, C.; Schini-Kerth, V.B.; Bronner, C.; et al. Induction of apoptosis by thymoquinone in lymphoblastic leukemia Jurkat cells is mediated by a p73-dependent pathway which targets the epigenetic integrator UHRF1. *Biochem. Pharmacol.* **2010**, *79*, 1251–1260. [[CrossRef](#)] [[PubMed](#)]
31. Abusnina, A.; Alhosin, M.; Keravis, T.; Muller, C.D.; Fuhrmann, G.; Bronner, C.; Lugnier, C. Down-regulation of cyclic nucleotide phosphodiesterase PDE1A is the key event of p73 and UHRF1 deregulation in thymoquinone-induced acute lymphoblastic leukemia cell apoptosis. *Cell. Signal.* **2011**, *23*, 152–160. [[CrossRef](#)] [[PubMed](#)]
32. Ke, X.; Zhao, Y.; Lu, X.; Wang, Z.; Liu, Y.; Ren, M.; Lu, G.; Zhang, D.; Sun, Z.; Xu, Z.; et al. TQ inhibits hepatocellular carcinoma growth in vitro and in vivo via repression of Notch signaling. *Oncotarget* **2015**, *6*, 32610–32621. [[CrossRef](#)] [[PubMed](#)]
33. El-Najjar, N.; Chatila, M.; Moukadem, H.; Vuorela, H.; Ocker, M.; Gandesiri, M.; Schneider-Stock, R.; Gali-Muhtasib, H. Reactive oxygen species mediate thymoquinone-induced apoptosis and activate ERK and JNK signaling. *Apoptosis* **2010**, *15*, 183–195. [[CrossRef](#)]
34. Pavlova, N.N.; Thompson, C.B. The Emerging Hallmarks of Cancer Metabolism. *Cell Metab.* **2016**, *23*, 27–47. [[CrossRef](#)] [[PubMed](#)]
35. Picard, M.; Wallace, D.C.; Burelle, Y. The rise of mitochondria in medicine. *Mitochondrion* **2016**, *30*, 105–116. [[CrossRef](#)] [[PubMed](#)]
36. Hoxhaj, G.; Manning, B.D. The PI3K-AKT network at the interface of oncogenic signalling and cancer metabolism. *Nat. Rev. Cancer* **2020**, *20*, 74–88. [[CrossRef](#)]
37. Chen, Z.; Lu, W.; Garcia-Prieto, C.; Huang, P. The Warburg effect and its cancer therapeutic implications. *J. Bioenerg. Biomembr.* **2007**, *39*, 267–274. [[CrossRef](#)] [[PubMed](#)]
38. Shi, T.; Ma, Y.; Cao, L.; Zhan, S.; Xu, Y.; Fu, F.; Liu, C.; Zhang, G.; Wang, Z.; Wang, R.; et al. B7-H3 promotes aerobic glycolysis and chemoresistance in colorectal cancer cells by regulating HK2. *Cell Death Dis.* **2019**, *10*, 308. [[CrossRef](#)] [[PubMed](#)]
39. Wolf, A.; Agnihotri, S.; Micallef, J.; Mukherjee, J.; Sabha, N.; Cairns, R.; Hawkins, C.; Guha, A. Hexokinase 2 is a key mediator of aerobic glycolysis and promotes tumor growth in human glioblastoma multiforme. *J. Exp. Med.* **2011**, *208*, 313–326. [[CrossRef](#)] [[PubMed](#)]
40. Mukherjee, A.; Ma, Y.; Yuan, F.; Gong, Y.; Fang, Z.; Mohamed, E.M.; Berrios, E.; Shao, H.; Fang, X. Lysophosphatidic Acid Up-Regulates Hexokinase II and Glycolysis to Promote Proliferation of Ovarian Cancer Cells. *Neoplasia* **2015**, *17*, 723–734. [[CrossRef](#)]
41. Coelho, R.G.; Calaça, I.C.; Celestrini, D.M.; Correia-Carneiro, A.H.; Costa, M.M.; Zancan, P.; Sola-Penna, M. Hexokinase and phosphofructokinase activity and intracellular distribution correlate with aggressiveness and invasiveness of human breast carcinoma. *Oncotarget* **2015**, *6*, 29375–29387. [[CrossRef](#)] [[PubMed](#)]
42. Zhang, Z.; Li, T.E.; Chen, M.; Xu, D.; Zhu, Y.; Hu, B.Y.; Lin, Z.F.; Pan, J.J.; Wang, X.; Wu, C.; et al. MFN1-dependent alteration of mitochondrial dynamics drives hepatocellular carcinoma metastasis by glucose metabolic reprogramming. *Br. J. Cancer* **2020**, *122*, 209–220. [[CrossRef](#)]
43. Torre, L.A.; Bray, F.; Siegel, R.L.; Ferlay, J.; Lortet-Tieulent, J.; Jemal, A. Global cancer statistics, 2012. *CA Cancer J. Clin.* **2015**, *65*, 87–108. [[CrossRef](#)] [[PubMed](#)]
44. Bray, F.; Ferlay, J.; Soerjomataram, I.; Siegel, R.L.; Torre, L.A.; Jemal, A. Global cancer statistics 2018: GLOBOCAN estimates of incidence and mortality worldwide for 36 cancers in 185 countries. *CA Cancer J. Clin.* **2018**, *68*, 394–424. [[CrossRef](#)] [[PubMed](#)]
45. Siegel, R.L.; Miller, K.D.; Fedewa, S.A.; Ahnen, D.J.; Meester, R.G.S.; Barzi, A.; Jemal, A. Colorectal cancer statistics, 2017. *CA Cancer J. Clin.* **2017**, *67*, 177–193. [[CrossRef](#)]
46. Anemone, A.; Consolino, L.; Conti, L.; Reineri, F.; Cavallo, F.; Aime, S.; Longo, D.L. In vivo evaluation of tumour acidosis for assessing the early metabolic response and onset of resistance to dichloroacetate by using magnetic resonance pH imaging. *Int. J. Oncol.* **2017**, *51*, 498–506. [[CrossRef](#)]
47. Brown, D.G.; Rao, S.; Weir, T.L.; O'Malia, J.; Bazan, M.; Brown, R.J.; Ryan, E.P. Metabolomics and metabolic pathway networks from human colorectal cancers, adjacent mucosa, and stool. *Cancer Metab.* **2016**, *4*, 11. [[CrossRef](#)] [[PubMed](#)]
48. Kareva, I. Prisoner's dilemma in cancer metabolism. *PLoS ONE* **2011**, *6*, e28576. [[CrossRef](#)]
49. Graziano, F.; Ruzzo, A.; Giacomini, E.; Ricciardi, T.; Aprile, G.; Loupakis, F.; Lorenzini, P.; Ongaro, E.; Zoratto, F.; Catalano, V.; et al. Glycolysis gene expression analysis and selective metabolic advantage in the clinical progression of colorectal cancer. *Pharm. J.* **2017**, *17*, 258–264. [[CrossRef](#)] [[PubMed](#)]
50. Lu, J. The Warburg metabolism fuels tumor metastasis. *Cancer Metastasis Rev.* **2019**, *38*, 157–164. [[CrossRef](#)] [[PubMed](#)]
51. Zhou, M.; Zhao, Y.; Ding, Y.; Liu, H.; Liu, Z.; Fodstad, O.; Riker, A.I.; Kamarajugadda, S.; Lu, J.; Owen, L.B.; et al. Warburg effect in chemosensitivity: Targeting lactate dehydrogenase-A re-sensitizes taxol-resistant cancer cells to taxol. *Mol. Cancer* **2010**, *9*, 33. [[CrossRef](#)] [[PubMed](#)]
52. Lu, C.W.; Lin, S.C.; Chen, K.F.; Lai, Y.Y.; Tsai, S.J. Induction of pyruvate dehydrogenase kinase-3 by hypoxia-inducible factor-1 promotes metabolic switch and drug resistance. *J. Biol. Chem.* **2008**, *283*, 28106–28114. [[CrossRef](#)] [[PubMed](#)]
53. Ganapathy-Kanniappan, S.; Geschwind, J.-F.H. Tumor glycolysis as a target for cancer therapy: Progress and prospects. *Mol. Cancer* **2013**, *12*, 152. [[CrossRef](#)] [[PubMed](#)]
54. Lundø, K.; Trauelsen, M.; Pedersen, S.F.; Schwartz, T.W. Why Warburg Works: Lactate Controls Immune Evasion through GPR81. *Cell Metab.* **2020**, *31*, 666–668. [[CrossRef](#)] [[PubMed](#)]

55. Cascone, T.; McKenzie, J.A.; Mbofung, R.M.; Punt, S.; Wang, Z.; Xu, C.; Williams, L.J.; Wang, Z.; Bristow, C.A.; Carugo, A.; et al. Increased Tumor Glycolysis Characterizes Immune Resistance to Adoptive T Cell Therapy. *Cell Metab.* **2018**, *27*, 977–987. [\[CrossRef\]](#)
56. Vander Heiden, M.G. Targeting cancer metabolism: A therapeutic window opens. *Nat. Rev. Drug Discov.* **2011**, *10*, 671–684. [\[CrossRef\]](#) [\[PubMed\]](#)
57. Tennant, D.A.; Durán, R.V.; Gottlieb, E. Targeting metabolic transformation for cancer therapy. *Nat. Rev. Cancer* **2010**, *10*, 267–277. [\[CrossRef\]](#) [\[PubMed\]](#)
58. Davidson, S.M.; Papagiannakopoulos, T.; Olenchock, B.A.; Heyman, J.E.; Keibler, M.A.; Luengo, A.; Bauer, M.R.; Jha, A.K.; O'Brien, J.P.; Pierce, K.A.; et al. Environment Impacts the Metabolic Dependencies of Ras-Driven Non-Small Cell Lung Cancer. *Cell Metab.* **2016**, *23*, 517–528. [\[CrossRef\]](#) [\[PubMed\]](#)
59. Owen, M.R.; Doran, E.; Halestrap, A.P. Evidence that metformin exerts its anti-diabetic effects through inhibition of complex 1 of the mitochondrial respiratory chain. *Biochem. J.* **2000**, *348 Pt 3*, 607–614. [\[CrossRef\]](#) [\[PubMed\]](#)
60. Wheaton, W.W.; Weinberg, S.E.; Hamanaka, R.B.; Soberanes, S.; Sullivan, L.B.; Anso, E.; Glasauer, A.; Dufour, E.; Mutlu, G.M.; Budigner, G.S.; et al. Metformin inhibits mitochondrial complex I of cancer cells to reduce tumorigenesis. *eLife* **2014**, *3*, e02242. [\[CrossRef\]](#)
61. Ben Sahra, I.; Laurent, K.; Giuliano, S.; Larbret, F.; Ponzio, G.; Gounon, P.; Le Marchand-Brustel, Y.; Giorgetti-Peraldi, S.; Cormont, M.; Bertolotto, C.; et al. Targeting cancer cell metabolism: The combination of metformin and 2-deoxyglucose induces p53-dependent apoptosis in prostate cancer cells. *Cancer Res.* **2010**, *70*, 2465–2475. [\[CrossRef\]](#) [\[PubMed\]](#)
62. Zhang, D.; Li, J.; Wang, F.; Hu, J.; Wang, S.; Sun, Y. 2-Deoxy-D-glucose targeting of glucose metabolism in cancer cells as a potential therapy. *Cancer Lett.* **2014**, *355*, 176–183. [\[CrossRef\]](#)
63. Wang, H.; Wang, L.; Zhang, Y.; Wang, J.; Deng, Y.; Lin, D. Inhibition of glycolytic enzyme hexokinase II (HK2) suppresses lung tumor growth. *Cancer Cell Int.* **2016**, *16*, 9. [\[CrossRef\]](#) [\[PubMed\]](#)
64. Lucantoni, F.; Düssmann, H.; Llorente-Folch, I.; Prehn, J.H.M. BCL2 and BCL(X)L selective inhibitors decrease mitochondrial ATP production in breast cancer cells and are synthetically lethal when combined with 2-deoxy-D-glucose. *Oncotarget* **2018**, *9*, 26046. [\[CrossRef\]](#) [\[PubMed\]](#)
65. Jha, M.K.; Suk, K. Pyruvate Dehydrogenase Kinase as a Potential Therapeutic Target for Malignant Gliomas. *Brain Tumor Res. Treat.* **2013**, *1*, 57–63. [\[CrossRef\]](#) [\[PubMed\]](#)
66. Caino, M.C.; Ghosh, J.C.; Chae, Y.C.; Vaira, V.; Rivadeneira, D.B.; Favarsani, A.; Rampini, P.; Kossenkov, A.V.; Aird, K.M.; Zhang, R.; et al. PI3K therapy reprograms mitochondrial trafficking to fuel tumor cell invasion. *Proc. Natl. Acad. Sci. USA* **2015**, *112*, 8638–8643. [\[CrossRef\]](#) [\[PubMed\]](#)
67. Mukherjee, A.K.; Basu, S.; Sarkar, N.; Ghosh, A.C. Advances in cancer therapy with plant based natural products. *Curr. Med. Chem.* **2001**, *8*, 1467–1486. [\[CrossRef\]](#) [\[PubMed\]](#)
68. Chikara, S.; Nagaprashantha, L.D.; Singhal, J.; Horne, D.; Awasthi, S.; Singhal, S.S. Oxidative stress and dietary phytochemicals: Role in cancer chemoprevention and treatment. *Cancer Lett.* **2018**, *413*, 122–134. [\[CrossRef\]](#) [\[PubMed\]](#)
69. Saunier, E.; Antonio, S.; Regazzetti, A.; Auzeil, N.; Laprévote, O.; Shay, J.W.; Coumoul, X.; Barouki, R.; Benelli, C.; Huc, L.; et al. Resveratrol reverses the Warburg effect by targeting the pyruvate dehydrogenase complex in colon cancer cells. *Sci. Rep.* **2017**, *7*, 6945. [\[CrossRef\]](#)
70. Rajput, S.; Kumar, B.N.P.; Dey, K.K.; Pal, I.; Parekh, A.; Mandal, M. Molecular targeting of Akt by thymoquinone promotes G(1) arrest through translation inhibition of cyclin D1 and induces apoptosis in breast cancer cells. *Life Sci.* **2013**, *93*, 783–790. [\[CrossRef\]](#) [\[PubMed\]](#)
71. Khan, M.A.; Tania, M.; Wei, C.; Mei, Z.; Fu, S.; Cheng, J.; Xu, J.; Fu, J. Thymoquinone inhibits cancer metastasis by downregulating TWIST1 expression to reduce epithelial to mesenchymal transition. *Oncotarget* **2015**, *6*, 19580–19591. [\[CrossRef\]](#) [\[PubMed\]](#)
72. Asaduzzaman Khan, M.; Tania, M.; Fu, S.; Fu, J. Thymoquinone, as an anticancer molecule: From basic research to clinical investigation. *Oncotarget* **2017**, *8*, 51907–51919. [\[CrossRef\]](#) [\[PubMed\]](#)
73. Gill, K.S.; Fernandes, P.; O'Donovan, T.R.; McKenna, S.L.; Doddakula, K.K.; Power, D.G.; Soden, D.M.; Forde, P.F. Glycolysis inhibition as a cancer treatment and its role in an anti-tumour immune response. *Biochim. Biophys. Acta* **2016**, *1866*, 87–105. [\[CrossRef\]](#) [\[PubMed\]](#)
74. Wu, J.; Hu, L.; Wu, F.; Zou, L.; He, T. Poor prognosis of hexokinase 2 overexpression in solid tumors of digestive system: A meta-analysis. *Oncotarget* **2017**, *8*, 32332–32344. [\[CrossRef\]](#) [\[PubMed\]](#)
75. Wang, Y.; Yun, Y.; Wu, B.; Wen, L.; Wen, M.; Yang, H.; Zhao, L.; Liu, W.; Huang, S.; Wen, N.; et al. FOXM1 promotes reprogramming of glucose metabolism in epithelial ovarian cancer cells via activation of GLUT1 and HK2 transcription. *Oncotarget* **2016**, *7*, 47985. [\[CrossRef\]](#) [\[PubMed\]](#)
76. Siveen, K.S.; Mustafa, N.; Li, F.; Kannaiyan, R.; Ahn, K.S.; Kumar, A.P.; Chng, W.J.; Sethi, G. Thymoquinone overcomes chemoresistance and enhances the anticancer effects of bortezomib through abrogation of NF-κB regulated gene products in multiple myeloma xenograft mouse model. *Oncotarget* **2014**, *5*, 634–648. [\[CrossRef\]](#) [\[PubMed\]](#)
77. Sutton, K.M.; Greenshields, A.L.; Hoskin, D.W. Thymoquinone, a bioactive component of black caraway seeds, causes G1 phase cell cycle arrest and apoptosis in triple-negative breast cancer cells with mutant p53. *Nutr. Cancer* **2014**, *66*, 408–418. [\[CrossRef\]](#) [\[PubMed\]](#)

78. Mu, G.G.; Zhang, L.L.; Li, H.Y.; Liao, Y.; Yu, H.G. Thymoquinone Pretreatment Overcomes the Insensitivity and Potentiates the Antitumor Effect of Gemcitabine Through Abrogation of Notch1, PI3K/Akt/mTOR Regulated Signaling Pathways in Pancreatic Cancer. *Dig. Dis. Sci.* **2015**, *60*, 1067–1080. [[CrossRef](#)] [[PubMed](#)]
79. El-Baba, C.; Mahadevan, V.; Fahlbusch, F.B.; Mohan, S.S.; Rau, T.T.; Gali-Muhtasib, H.; Schneider-Stock, R. Thymoquinone-induced conformational changes of PAK1 interrupt prosurvival MEK-ERK signaling in colorectal cancer. *Mol. Cancer* **2014**, *13*, 201. [[CrossRef](#)]
80. Yang, J.; Kuang, X.R.; Lv, P.T.; Yan, X.X. Thymoquinone inhibits proliferation and invasion of human nonsmall-cell lung cancer cells via ERK pathway. *Tumour Biol.* **2015**, *36*, 259–269. [[CrossRef](#)]
81. Lee, Y.M.; Kim, G.H.; Park, E.J.; Oh, T.I.; Lee, S.; Kan, S.Y.; Kang, H.; Kim, B.M.; Kim, J.H.; Lim, J.H. Thymoquinone Selectively Kills Hypoxic Renal Cancer Cells by Suppressing HIF-1 $\alpha$ -Mediated Glycolysis. *Int. J. Mol. Sci.* **2019**, *20*, 1092. [[CrossRef](#)] [[PubMed](#)]
82. Pandita, A.; Kumar, B.; Manvati, S.; Vaishnavi, S.; Singh, S.K.; Bamezai, R.N. Synergistic combination of gemcitabine and dietary molecule induces apoptosis in pancreatic cancer cells and down regulates PKM2 expression. *PLoS ONE* **2014**, *9*, e107154. [[CrossRef](#)] [[PubMed](#)]
83. Zhang, J.; Yu, X.H.; Yan, Y.G.; Wang, C.; Wang, W.J. PI3K/Akt signaling in osteosarcoma. *Clin. Chim. Acta* **2015**, *444*, 182–192. [[CrossRef](#)] [[PubMed](#)]
84. Danielsen, S.A.; Eide, P.W.; Nesbakken, A.; Guren, T.; Leithe, E.; Lothe, R.A. Portrait of the PI3K/AKT pathway in colorectal cancer. *Biochim. Biophys. Acta* **2015**, *1855*, 104–121. [[CrossRef](#)] [[PubMed](#)]
85. Narayanankutty, A. PI3K/ Akt/ mTOR Pathway as a Therapeutic Target for Colorectal Cancer: A Review of Preclinical and Clinical Evidence. *Curr. Drug Targets* **2019**, *20*, 1217–1226. [[CrossRef](#)] [[PubMed](#)]
86. Rathmell, J.C.; Fox, C.J.; Plas, D.R.; Hammerman, P.S.; Cinalli, R.M.; Thompson, C.B. Akt-directed glucose metabolism can prevent Bax conformation change and promote growth factor-independent survival. *Mol. Cell. Biol.* **2003**, *23*, 7315–7328. [[CrossRef](#)]
87. Elstrom, R.L.; Bauer, D.E.; Buzzai, M.; Karnauskas, R.; Harris, M.H.; Plas, D.R.; Zhuang, H.; Cinalli, R.M.; Alavi, A.; Rudin, C.M.; et al. Akt stimulates aerobic glycolysis in cancer cells. *Cancer Res.* **2004**, *64*, 3892–3899. [[CrossRef](#)] [[PubMed](#)]
88. Gottlob, K.; Majewski, N.; Kennedy, S.; Kandel, E.; Robey, R.B.; Hay, N. Inhibition of early apoptotic events by Akt/PKB is dependent on the first committed step of glycolysis and mitochondrial hexokinase. *Genes Dev.* **2001**, *15*, 1406–1418. [[CrossRef](#)] [[PubMed](#)]
89. Plas, D.R.; Talapatra, S.; Edinger, A.L.; Rathmell, J.C.; Thompson, C.B. Akt and Bcl-xL promote growth factor-independent survival through distinct effects on mitochondrial physiology. *J. Biol. Chem.* **2001**, *276*, 12041–12048. [[CrossRef](#)] [[PubMed](#)]
90. Edinger, A.L.; Thompson, C.B. Antigen-presenting cells control T cell proliferation by regulating amino acid availability. *Proc. Natl. Acad. Sci. USA* **2002**, *99*, 1107–1109. [[CrossRef](#)] [[PubMed](#)]
91. Buzzai, M.; Bauer, D.E.; Jones, R.G.; DeBerardinis, R.J.; Hatzivassiliou, G.; Elstrom, R.L.; Thompson, C.B. The glucose dependence of Akt-transformed cells can be reversed by pharmacologic activation of fatty acid  $\beta$ -oxidation. *Oncogene* **2005**, *24*, 4165–4173. [[CrossRef](#)]
92. Koppenol, W.H.; Bounds, P.L.; Dang, C.V. Otto Warburg's contributions to current concepts of cancer metabolism. *Nat. Rev. Cancer* **2011**, *11*, 325–337. [[CrossRef](#)] [[PubMed](#)]
93. Patra, K.C.; Hay, N. The pentose phosphate pathway and cancer. *Trends Biochem. Sci.* **2014**, *39*, 347–354. [[CrossRef](#)] [[PubMed](#)]
94. Nilsson, R.; Jain, M.; Madhusudhan, N.; Sheppard, N.G.; Strittmatter, L.; Kampf, C.; Huang, J.; Asplund, A.; Mootha, V.K. Metabolic enzyme expression highlights a key role for MTHFD2 and the mitochondrial folate pathway in cancer. *Nat. Commun.* **2014**, *5*, 3128. [[CrossRef](#)] [[PubMed](#)]
95. Locasale, J.W. Serine, glycine and one-carbon units: Cancer metabolism in full circle. *Nat. Rev. Cancer* **2013**, *13*, 572–583. [[CrossRef](#)] [[PubMed](#)]
96. Gupta, G.P.; Massagué, J. Cancer metastasis: Building a framework. *Cell* **2006**, *127*, 679–695. [[CrossRef](#)]
97. Vaquero, J.; Guedj, N.; Clapéron, A.; Nguyen Ho-Bouloires, T.H.; Paradis, V.; Fouassier, L. Epithelial-mesenchymal transition in cholangiocarcinoma: From clinical evidence to regulatory networks. *J. Hepatol.* **2017**, *66*, 424–441. [[CrossRef](#)] [[PubMed](#)]
98. Cho, S.J.; Yoon, C.; Lee, J.H.; Chang, K.K.; Lin, J.X.; Kim, Y.H.; Kook, M.C.; Aksoy, B.A.; Park, D.J.; Ashktorab, H.; et al. KMT2C Mutations in Diffuse-Type Gastric Adenocarcinoma Promote Epithelial-to-Mesenchymal Transition. *Clin. Cancer Res.* **2018**, *24*, 6556–6569. [[CrossRef](#)] [[PubMed](#)]
99. Sjöberg, E.; Meyrath, M.; Milde, L.; Herrera, M.; Lötvrot, J.; Hägerstrand, D.; Frings, O.; Bartish, M.; Rolny, C.; Sonnhammer, E.; et al. A Novel ACKR2-Dependent Role of Fibroblast-Derived CXCL14 in Epithelial-to-Mesenchymal Transition and Metastasis of Breast Cancer. *Clin. Cancer Res.* **2019**, *25*, 3702–3717. [[CrossRef](#)]
100. Bylsma, L.C.; Gillezeau, C.; Garawin, T.A.; Kelsh, M.A.; Fryzek, J.P.; Sangaré, L.; Lowe, K.A. Prevalence of RAS and BRAF mutations in metastatic colorectal cancer patients by tumor sidedness: A systematic review and meta-analysis. *Cancer Med.* **2020**, *9*, 1044–1057. [[CrossRef](#)] [[PubMed](#)]
101. Robert, C.; Karaszewska, B.; Schachter, J.; Rutkowski, P.; Mackiewicz, A.; Stroiakovski, D.; Lichinitser, M.; Dummer, R.; Grange, F.; Mortier, L.; et al. Improved overall survival in melanoma with combined dabrafenib and trametinib. *N. Engl. J. Med.* **2015**, *372*, 30–39. [[CrossRef](#)] [[PubMed](#)]

102. Zhang, Y.; Fan, Y.; Huang, S.; Wang, G.; Han, R.; Lei, F.; Luo, A.; Jing, X.; Zhao, L.; Gu, S.; et al. Thymoquinone inhibits the metastasis of renal cell cancer cells by inducing autophagy via AMPK/mTOR signaling pathway. *Cancer Sci.* **2018**, *109*, 3865–3873. [[CrossRef](#)] [[PubMed](#)]
103. Shanmugam, M.K.; Ahn, K.S.; Hsu, A.; Woo, C.C.; Yuan, Y.; Tan, K.H.B.; Chinnathambi, A.; Alahmadi, T.A.; Alharbi, S.A.; Koh, A.P.F.; et al. Thymoquinone Inhibits Bone Metastasis of Breast Cancer Cells Through Abrogation of the CXCR4 Signaling Axis. *Front. Pharmacol.* **2018**, *9*, 1294. [[CrossRef](#)] [[PubMed](#)]
104. Patra, K.C.; Wang, Q.; Bhaskar, P.T.; Miller, L.; Wang, Z.; Wheaton, W.; Chandel, N.; Laakso, M.; Muller, W.J.; Allen, E.L.; et al. Hexokinase 2 is required for tumor initiation and maintenance and its systemic deletion is therapeutic in mouse models of cancer. *Cancer Cell* **2013**, *24*, 213–228. [[CrossRef](#)] [[PubMed](#)]
105. Wenes, M.; Shang, M.; Di Matteo, M.; Goveia, J.; Martín-Pérez, R.; Serneels, J.; Prenen, H.; Ghesquière, B.; Carmeliet, P.; Mazzone, M. Macrophage Metabolism Controls Tumor Blood Vessel Morphogenesis and Metastasis. *Cell Metab.* **2016**, *24*, 701–715. [[CrossRef](#)] [[PubMed](#)]
106. Bhattacharya, D.; Scimè, A. Metabolic Regulation of Epithelial to Mesenchymal Transition: Implications for Endocrine Cancer. *Front. Endocrinol.* **2019**, *10*, 773. [[CrossRef](#)] [[PubMed](#)]
107. Gui, D.Y.; Sullivan, L.B.; Luengo, A.; Hosios, A.M.; Bush, L.N.; Gitego, N.; Davidson, S.M.; Freinkman, E.; Thomas, C.J.; Vander Heiden, M.G. Environment dictates dependence on mitochondrial complex I for NAD<sup>+</sup> and aspartate production and determines cancer cell sensitivity to metformin. *Cell Metab.* **2016**, *24*, 716–727. [[CrossRef](#)] [[PubMed](#)]
108. Peng, F.; Wang, J.H.; Fan, W.J.; Meng, Y.T.; Li, M.M.; Li, T.T.; Cui, B.; Wang, H.F.; Zhao, Y.; An, F.; et al. Glycolysis gatekeeper PDK1 reprograms breast cancer stem cells under hypoxia. *Oncogene* **2018**, *37*, 1062–1074. [[CrossRef](#)] [[PubMed](#)]